HHS Public Access

Author manuscript

Cell Rep. Author manuscript; available in PMC 2016 August 30.

Published in final edited form as:

Cell Rep. 2014 May 8; 7(3): 623–633. doi:10.1016/j.celrep.2014.03.063.

Pkd1 regulates lymphatic vascular morphogenesis during development

Baptiste Coxam[1], **Amélie Sabine**[2], **Neil I. Bower**[1], **Kelly A. Smith**[1], **Cathy Pichol-Thievend**[1], **Renae Skoczylas**[1], **Jonathan W. Astin**[3], **Emmanuelle Frampton**[1], **Muriel Jaquet**[2], **Philip S. Crosier**[3], **Robert G. Parton**[1], **Natasha L. Harvey**[4], **Tatiana V. Petrova**[2], **Stefan Schulte-Merker**[5], **Mathias Francois**[1,*], and **Benjamin M. Hogan**[1,*,#]

[1]Institute for Molecular Bioscience, The University of Queensland, Brisbane, QLD 4072, Australia
[2]Department of Oncology, University Hospital of Lausanne, and Department of Biochemistry, University of Lausanne, 1066 Epalinges, Switzerland [3]Department of Molecular Medicine and Pathology, School of Medical Sciences, The University of Auckland, 1142 Auckland, New Zealand
[4]Division of Haematology, Centre for Cancer Biology, SA Pathology, Adelaide, SA 5000, Australia
[5]Hubrecht Institute-KNAW & UMC Utrecht, 3584CT Utrecht, The Netherlands

Abstract

Lymphatic vessels arise during development through sprouting of precursor cells from veins, which is regulated by well-studied signaling and transcriptional mechanisms. Less well understood is the ongoing elaboration of vessels to form a network. This involves cell polarisation, coordinated migration, adhesion, mixing, regression and cell shape rearrangements. We identified a zebrafish mutant, *lymphatic and cardiac defects 1 (lyc1),* with reduced lymphatic vessel development. We found a mutation in *polycystic kidney disease 1a* to be responsible for the phenotype. *PKD1* is the most frequently mutated gene in autosomal dominant polycystic kidney disease (ADPKD). Initial sprouting of lymphatic precursors is normal in *lyc1* mutants, but ongoing migration fails. Loss of *Pkd1* in mice also has no effect on sprouting of precursors but leads to failed morphogenesis of the subcutaneous lymphatic network. Individual lymphatic endothelial cells display defective polarity, elongation and adherens junctions. This work identifies a highly selective and unexpected role for *Pkd1* in lymphatic vessel morphogenesis during development.

Introduction

Lymphatic vessels form in the developing embryo as a result of specification of lymphatic endothelial cell (LEC) fate, followed by coordinated cellular sprouting, morphogenesis and network elaboration. LEC fate is specified through key transcription factors SOX18,

[#]Corresponding author: Dr Ben Hogan, Division of Molecular Genetics and Development, Institute for Molecular Bioscience, University of Queensland, St Lucia, 4072 QLD, AUSTRALIA, b.hogan@imb.uq.edu.au.
[*]Joint last authors

SUPPLEMENTAL INFORMATION
Supplemental information includes 10 figures, 7 movies and Supplemental Experimental Procedures.

COUPTFII and PROX1, which act initially in the veins (Francois et al., 2008, Wigle and Oliver, 1999, Srinivasan et al., 2010). LEC precursors subsequently sprout from the veins and migrate through the embryonic environment (reviewed in (Koltowska et al., 2013)). This process is under the control of VEGFC/VEGFR3 signaling and its modulators (Yuan et al., 2002, Wang et al., 2010, Galvagni et al., 2010, Chen et al., 2010, Mäkinen et al., 2001, Karkkainen et al., 2004). In mouse, lymphatic precursors form lymph sacs in the anterior of the embryo, which likely remodel into major lymphatic vessels (Hagerling et al., 2013, François et al., 2012). Superficial LECs (sLECs) migrate dorsally as loosely attached individual cells to form the sub-cutaneous lymphatic network (Hagerling et al., 2013, Yang et al., 2012). While several guidance molecules, cellular interactions, and extrinsic forces pattern embryonic lymphangiogenesis (reviewed in (Koltowska et al., 2013), much remains to be understood about the cellular mechanisms that regulate LEC polarization, adhesion, outgrowth, remodeling and morphogenesis.

In zebrafish, there are strong parallels with mammals in the molecular and cellular processes that regulate lymphatic vascular development (Yaniv et al., 2006, Kuchler et al., 2006, Hogan et al., 2009b). We identified a novel zebrafish mutant that fails to form lymphatic vessels. This mutant uncovered a surprising role for the ADPKD gene *Pkd1* in lymphatic vascular development. We find that *Pkd1* regulates cell polarity, elongation and adherens junctions in sprouting lymphatic vessels during embryonic network formation. This function of *Pkd1* is conserved between mice and zebrafish and cell autonomous in endothelial knockout mice. Our findings suggest a uniquely staged role for PKD1 in the regulation of lymphatic vascular morphogenesis.

Results

lymphatic and cardiac defects 1 mutants fail to form a lymphatic vasculature

In a screen for zebrafish lymphatic vascular mutants, we identified a mutant dubbed *lymphatic and cardiac defects 1* (*lyc1*). *lyc1* mutants exhibited a reduction or loss of the main axial lymphatic vessel, the thoracic duct (TD) at 4 days post fertilization (dpf), as well as mild cardiac oedema, but retained blood circulation (Figure 1A–B, C–D, I, Movies S1–2). By 5 dpf, mutant blood flow was reduced and cardiac oedema increased in severity (Figure S1, data not shown). To determine the origins of the phenotype, we first examined gene expression for arterio-venous genes, lymphangiogenesis regulators (including chemokines and receptors) and flow-induced pathways at 32 hours post fertilisation (hpf), during the initiation of lymphatic development. These markers were unchanged in *lyc1* embryos (Figure S2). In the zebrafish, precursor LECs emerge from the posterior cardinal vein (PCV) and migrate dorsally to the horizontal myoseptum to form parachordal lymphangioblasts (PLs). Additional venous sprouts form intersegmental veins (vISVs). Strikingly, the numbers of both vISVs and PLs were normal in *lyc1* mutants (Figure 1E–H, J & K).

This phenotype differs significantly from previously characterized lymphatic mutants for *vegfc*, *vegfr3* or *ccbe1* (Hogan et al., 2009a, Hogan et al., 2009b, Villefranc et al., 2013, Le Guen et al., 2014), which lack all venous sprouting. Time-lapse analysis showed that the lymphatic defect resulted from a block in the migration of PLs out of the horizontal myoseptum (Movies S3–S4). Quantitative analysis of cell behavior spanning this earliest

period of altered migration, revealed that mutant precursor LECs remain mobile within the myoseptum but show altered exploratory behavior and filopodial extension dynamics consistent with impaired directional migration (Movies S5 and S6, Figure S3).

A loss-of-function mutation in *pkd1a* is responsible for the *lyc1* phenotype

Meiotic mapping (see methods) was used to identify a region of Chromosome 1 containing the *lyc1* locus. The critical interval (Figure 2A) contained two genes, *tuberous sclerosis 2 (tsc2)* and *polycystic kidney disease Ia (pkd1a*). Sequencing revealed a mutation in *pkd1a*, introducing a premature stop codon (R3607X) (Figure 2B). This mutation was predicted to result in the failed translation of six of the eleven transmembrane domains and essential C-terminal cytoplasmic tail of the protein.

In the zebrafish genome, *pkd1* (encoding Polycystin1) is present as duplicate genes, with *pkd1a* coding for a conserved 4281 amino acid protein.. In mammals, POLYCYSTIN1 protein localises to primary cilia, apical membranes, adherens and desmosomal junctions. It can act as a mechanosensory signaling protein, transducing extracellular signals through its cytoplasmic C-terminal domain (reviewed in (Zhou, 2009)). POLYCYSTIN1 binds to POLYCYSTIN2 (a calcium pump) at the membrane to regulate Ca^{2+} influx and signaling but also binds to E-CADHERIN, β-CATENIN and components of the planar cell polarity pathway (Castelli et al., 2013, Lal et al., 2008, Geng et al., 2000, Boca et al., 2007, Roitbak et al., 2004). In humans, *PKD1* and *PKD2* (encoding POLYCYSTIN2) are the most commonly mutated genes in ADPKD with roles in the regulation of kidney epithelial cell polarity, morphogenesis and cystogenesis (for review (Zhou, 2009, Chapin and Caplan, 2010)). Interestingly, *PKD1* haploinsufficiency and loss-of-function has been associated with cardiovascular complications in mice and humans (reviewed in (Rossetti and Harris, 2013)).

Previous studies investigating the consequences of depleting Polycystin1 (a and b) in zebrafish, found that *MO-pkd1a/b* embryos exhibit a specific body curvature phenotype (Mangos et al., 2010). We injected *MO-pkd1b* into our putative *pkd1a* mutant embryos and robustly induced this phenotype, confirming that the *lyc1* mutation is a *pkd1a* loss-of-function allele (Figure 2C and Figure S4). Pkd1 and Pkd2 can modulate extracellular matrix (ECM) formation (Mangos et al., 2010). Importantly, even the most phenotypically penetrant *lyc1 (pkd1a)* mutants for lymphangiogenesis do not display body curvature defects associated with altered ECM. We examined several markers and knockdown scenarios but found no evidence for increased ECM or a role of altered matrix in the *lyc1* lymphatic phenotype (Figure S5).

pkd1a is expressed in migrating LECs and loss-of-function in the ADPKD complex mimics *lyc1* defects

We found that *pkd1a* expression was ubiquitous in the 24 hpf embryo but enriched in the trunk during secondary sprouting at 32hpf (Figure 2D). We saw no evidence for nonsense-mediated decay in mutants using *in situ* hybridization at 32 hpf (n=130 embryos analysed from a heterozygous incross, data not shown). As *in situ* hybridization has proven insensitive to detect transcripts in LECs in older zebrafish (post 3 dpf), we isolated LECs from zebrafish

embryos using FACs. Taking advantage of a new transgenic line *Tg(lyve1:DsRed2)*^{nz101} (Okuda et al., 2012) labeling embryonic veins and lymphatic vessels, crossed onto the *Tg(kdrl:egfp)*^{s843} line (restricted to blood vessels (Jin et al., 2005)), we isolated LECs and venous ECs (VECs). We performed Q-PCR for known markers of LECs and VECs, validating the specificity of cell populations (Figure 2E, Figure S4). *pkd1a* and *pkd2* were expressed in VECs and LECs, with *pkd1a* in both at 3dpf but reduced in LECs relative to BECs at 5 dpf. *pkd1b* was found at low levels, almost undetectable at all stages analysed (Figure 2F, Figure S4). This analysis confirmed expression of *pkd1a* and *pkd2* in the relevant endothelial cells at the stages affected in the *lyc1* mutant.

In endothelial cells, POLYCYSTIN1 can act through the regulation of intra- and extra-cellular entry of calcium ions through POLYCYSTIN2 (Nauli et al., 2003, Chapin and Caplan, 2010). To investigate if this mechanism may regulate lymphangiogenesis, we knocked down Pkd2. Embryos depleted for Pkd2 exhibited a gross phenotype similar to that of *lyc1/MO-pkd1b* embryos and a reduction in thoracic duct extent (Figure 2G–I, Figure S4). To determine if Ca^{2+} signaling may be involved, we treated embryos with a Ca^{2+}channel blocker and a Ca^{2+} channel agonist that have been previously validated in zebrafish (North et al., 2009). These treatments in wildtype and mutant animals generated phenotypes that were highly reminiscent of the *lyc1* phenotype (Figure S4). Cacna1s, an L-type calcium channel that is targeted by Nifedipine, was validated as expressed in ECs by Q-PCR (Figure S4). Taken together, these correlative phenotypes are consistent with Pkd1 functioning as a component of the canonical ADPKD complex.

Pkd1 cell-autonomously regulates development of the sub-cutaneous lymphatic vascular network in mice

While most previous studies in mammalian models focus on the role of *Pkd1* in epithelia, *Pkd1* null mice have been shown to exhibit cardiovascular, skeletal and renal defects (Kim et al., 2000, Piontek et al., 2004, Boulter et al., 2001). Embryos devoid of *Pkd1* die after 15.5 dpc displaying severe hemorrhaging and subcutaneous oedema (Kim et al., 2000, Muto et al., 2002) but a role for this gene in lymphangiogenesis has yet to be reported.

We generated *Pkd1* knockout embryos and examined their overall morphology. We observed the previously described subcutaneous oedema, but not hemorrhaging (Figure 3A–C). Embryonic lymph sacs were present but were blood filled in *Pkd1* KO embryos (Figure 3D–I). This phenotype suggests that lymphatics in this mutant would not sustain fluid drainage and may explain the sub-cutaneous oedema. Interestingly, we did not find any gross defect in lymphovenous valves in *Pkd1* KO embryos at 14.5 dpc (Figure S6) perhaps suggesting that blood enters the lymphatic vasculature early during morphogenesis, before valve maturation (François et al., 2012). We next examined the developing subcutaneous lymphatic vasculature in dorsal embryonic skin, a useful system to quantify lymphatic vascular phenotypes (Kartopawiro et al., 2013, James et al., 2013). We found that *Pkd1* KO embryos exhibit defects in the remodeling and morphogenesis of the lymphatic network, with increased width of sprouting vessels, increased cell number per vessel and a significant reduction in network branching (Figure 3L, M, R, T, U).

Previous studies reported that *Tie2:Cre* mediated deletion of *Pkd1* did not lead to vascular abnormalities and these knockout mice did not display the oedema observed in the full knockout animals (Hassane et al., 2010, Garcia-Gonzalez et al., 2010). This implies that the phenotypes that we observed may not reflect function within the endothelial cells themselves. To investigate this further, we crossed the *Tie2:Cre* strain into a *ROSA26r*-LacZ background, and examined the activity of Cre in the sub-cutaneous lymphatic vasculature. While active in the blood vascular endothelium, we could not detect β-Galactosidase throughout the lymphatic vasculature (Figure S7). This indicates that previous work could not have uncovered a function for *Pkd1* in these vessels. We generated knockout embryos for *Pkd1* using *Tie2:Cre* and found that these embryos had no phenotype in their subcutaneous lymphatic vessels (Figure S8). Hence, we next utilized *Sox18:GFP-Cre-ErT2(GCE)* as an additional endothelial CRE strain (Kartopawiro et al., 2013). We validated the use of *Sox18:GCE* on a *Rosa26r*-LacZ background, which demonstrated activity throughout the embryonic vasculature (Figure S7). We also used a CRE-inducible *tdTomato* reporter, which allowed us to quantify activity in subcutaneous lymphatics by co-staining with LEC markers NRP2 and PROX1. We found that induced *Sox18:GCE* was active in 58% of sprouting subcutaneous LECs at 13.5 dpc and frequently in clonal regions spanning whole sprouts and vessels (Figure 3J,K, Figure S7H–Q, Movie S7).

We generated induced *Pkd1* endothelial cell knockout (iΔECKO) embryos using this line. *Pkd1*$^{\text{iΔECKO}}$ embryos displayed either mild or no subcutaneous oedema at 14.5 dpc (Figure 3C), with lymph sacs present but not containing blood (Figure 3I, F). In the subcutaneous lymphatic vasculature, *Pkd1*^{iΔECKO} embryos displayed similar defects to germline KO animals if marginally milder based on quantification (Figure 3N,Q, T, U). We also examined the blood vasculature of *Pkd1* KO embryos. While we saw defects in germline KO embryos, these were at the dorsal midline associated with oedema and thus considered secondary to altered tissue architecture (Figure S6). In contrast, iΔECKO embryos displayed normal blood vasculature at 14.5 dpc, including normal vessel width and branching (Figure S6). Interestingly, endothelial KO embryos did not show reduced LEC migration towards the midline (Figure 3N). This would be expected for known pathways such as VEGFC/VEGFR3 signaling and may suggest that PKD1 functions through a previously uncharacterized mechanism.

PKD1 regulates sprouting and cell-cell junctions *in vitro* in human lymphatic endothelial cells

We next examined the sprouting of human LECs *in vitro* in response to VEGFC using a spheroid outgrowth assay. Spheroids extend multicellular sprouts in response to VEGFC. siRNA mediated knockdown of *PKD1* in LECs resulted in a reduced number of cells within these sprouts, with extensions exhibiting reduced length and abnormal morphology (Figure 4A–H, Figure S9). The efficacy of knockdown with the siRNA mix was validated by Q-PCR and the specificity of this phenotype was verified with independent knockdown using an shRNA approach (Figure S9).

We examined the phenotype of LECs in cultured monolayers and observed a rapid change in morphology following *PKD1* knockdown (Figure 4I–P). Analysis of F-actin indicated that

stress fibers were disorganized in these cells (Figure 4I, M). Furthermore, analysis of the cell junctions revealed that VE-CADHERIN and β-CATENIN were reduced and disorganized at junctions following Pkd1 knockdown (Figure 4J–K, N–O). ZO-1 localisation at tight junctions was relatively unaffected in these assays, despite altered cell morphology, suggesting a level of selectivity to adherens junctions (Figure 4L, P). The levels of VE-CADHERIN were not altered by western blot although β-CATENIN showed a mild reduction (Figure S9) probably indicative of generally destablised junctional complexes.

Pkd1 regulates polarity and cell-cell junctions during lymphatic vessel morphogenesis in mice

Pkd1 has been implicated in the regulation of polarity in epithelial cells and shown to regulate cellular convergent extension and polarity during kidney tubule morphogenesis through planar cell polarity (PCP) signaling (Castelli et al., 2013). PKD1 binds to PAR3, aPKC as well as E-CADHERIN and β-CATENIN in epithelial cells, therefore being associated with both polarity and junctional components (Castelli et al., 2013, Lal et al., 2008, Geng et al., 2000, Boca et al., 2007, Roitbak et al., 2004). Recently, the PCP pathway has been shown to regulate junctional rearrangements in developing LECs, at least during the process of valve morphogenesis (Tatin et al., 2013).

To determine whether polarity and/or cell junctions play a role in *Pkd1*-mediated vascular phenotypes, we examined cell polarity in sprouting embryonic lymphatic vessels. The Golgi apparatus orients toward the migration front relative to the nucleus in many cell types including in wildtype LECs at 14.5 dpc (Figure 5A, C), hence serving as an ideal readout for cell polarity. We quantified Golgi orientation in *Pkd1* KO embryos and found it to be significantly randomized in 14.5 dpc lymphatic vessels (Figure 5A–D, G). Furthermore, this loss of polarity was associated with increased nucleus sphericity in mutant vessels, which is a previously described proxy for polarity and migratory behavior (Hagerling et al., 2013) (Figure 5H).

To determine the earliest defect, we performed detailed phenotypic analysis at 10.5 and 11.5 dpc. At 10.5 dpc, analysis of PROX1 expression indicated that cell migration from the cardinal vein and nuclear morphology was normal in mutants (Figure 5I, S6G–H). However, at 11.5dpc, while the blood vasculature was grossly normal (Figure S6), mutant LECs at the sprouting vessel front displayed significantly increased nucleus sphericity (decreased elipticity) compared with wild type (Figure 5J). We assessed Golgi orientation at these stages but the direction of individual cell migration events was not regular and the midline cannot be used as a direction of migration until later in development (data not shown). These early (11.5 dpc) leading vessels also exhibited morphology similar to later $Pkd1^{KO}$ vessels with increased sprout width and numbers of nuclei/sprout length (Figure S6I–J).

Finally, we investigated cell shape and the morphology of junctions within lymphatic vessels. At 14.5 dpc, VE-CADHERIN expression highlighted cell shape and showed that mutant cells failed to elongate along the plane of migration towards the midline compared with wildtype vessels (Figure 5K–L, O–P, S). At the level of individual junctional morphology, both VE-CADHERIN and β-CATENIN expression identified junctions that displayed immature morphology with irregular intracellular protrusions (arrowheads Figure

5M, N, Q, R). These phenotypes were only associated with phenotypically mutant vessels and not wildtype morphologies in mutant embryos (data not shown), note the phenotypic variability in Figure 3. Quantification of the number of cells displaying immature junctions per vessel demonstrated a significant phenotype at 14.5 and 12.5 dpc (Figure 5T–V). These phenotypes are highly reminiscent of those observed in *Pkd1* mutants in the kidney tubules (Castelli et al., 2013).

Discussion

Our results demonstrate the surprising finding that *Pkd1* is a regulator of lymphatic vessel development. In zebrafish, at the cellular level, Pkd1 regulates LEC migration out of the horizontal myoseptum but not initial sprouting from veins that is regulated by *ccbe1*/*vegfc*/*vegfr3* (Hogan et al., 2009a, Hogan et al., 2009b, Le Guen et al., 2014, Villefranc et al., 2013). *pkd1a* is expressed in lymphatic precursor cells when they are actively migrating, consistent with the earliest cellular defects in the mutant.

It was important given the highly studied nature of Pkd1 to ask if this function was conserved in mammals. In knockout mice, early specification and initial sprouting of LECs occurs normally. However, defects are seen in the morphology of migrating LECs in the embryo at 11.5 dpc with morphological defects in the subcutaneous lymphatic network prominent by 14.5 dpc. This uniquely timed requirement is distinct from phenotypes in known pathways, suggesting that *Pkd1* may regulate uncharacterised processes in developing LECs. Interestingly, the lymph sacs were blood filled in the full knockout but not in the endothelial knockout, which displayed only mild oedema. This may be due to the staging of tamoxifen treatment to knockout *Pkd1* function from 9.5 or 11.5 dpc, when lymph sacs are already establishing (Hagerling et al., 2013). Alternatively, it may suggest a non-endothelial contribution that remains uncharacterised. The observation that the lymphatic phenotype was visible in *Sox18:GCE,* which acts in LECs, but not the *Tie2:Cre* strain, which we observed acts in BECs in the skin, suggests that deletion in LECs themselves is responsible for the lymphatic morphogenesis defect.

Given the diverse functions of the protein, several hypotheses could explain the observed migration and morphogenesis defects in *Pkd1* loss-of-function models. PKD1 has been previously reported to function at the primary cilium in endothelial cells (Nauli et al., 2008). However, we found lymphatic vessels developed normally in a ciliogenesis mutant (*ift88* (Huang and Schier, 2009)), we saw no evidence for altered ciliogenesis in *lyc1* mutants and overexpression of a Pkd1a-YFP fusion protein driven by the *pkd1a* promoter (BAC clone) did not lead to cilium enrichment (Figure S10). Hence, we find no supportive evidence that the function of Pkd1 in zebrafish lymphatic development occurs at the cilium. As Pkd1 can also localize to adherens junctions, desmosomal junctions, intracellular organelles and has a number of binding partners, it has potential to act at diverse locations.

The earliest consequences of loss-of-function are changes in cell morphology during morphogenesis, including altered polarity and adhesion. Cell polarity and adhesion are intimately associated and must be carefully regulated to control tissue morphogenesis. It is hard to determine which defect is primarily regulated by *Pkd1*. However, parallels can be

drawn with recent findings where Pkd1 regulates cellular convergent extension during tube formation through the PCP pathway (Castelli et al., 2013). While it will take further work to delineate the pathways modulated by *Pkd1* in LECs, the finding of a crucial role in lymphatic vascular development is unexpected and serves as a unique entry point to understand lymphatic vascular morphogenesis.

Experimental procedures

Zebrafish strains, mapping and genotyping

All animal use conformed to ethical guidelines of the animal ethics committee at the University of Queensland. Zebrafish were maintained and screening performed as previously described (Hogan et al., 2009a). Mapping and genotyping was performed as previously described (Hogan et al., 2009a) with details of primers given in Supplemental Experimental Procedures.

The *Tg(kdrl:egfp)*^{s843}, *Tg(fli1a:EGFP)*^{y1}, *Tg(-6.5kdrl:mcherry)*^{s916}, *Tg(-0.8flt1:tdTomato), Tg(lyve1:DsRed2)*^{nz101} lines were previously described (Hogan et al., 2009b, Lawson and Weinstein, 2002, Bussmann et al., 2010, Okuda et al., 2012, Jin et al., 2005).

Mouse strains

We generated *Sox18:GFP-Cre-ErT2(GCE), B6.129S4-Pkd1*$^{tm2Ggg/J}$ *(Pkd1*$^{f/f}$*); Rosa26rLacZ* (C57BL/6 background) mice by crossing *Pkd1*$^{f/f}$ mice to both *Rosa26rLacZ* and *Sox18:GFP-Cre-ErT2* mice and crossing resulting carriers. We generated *Tie2:Cre, Rosa26rLacZ* (C57BL/6 background) mice by crossing *Tie2:Cre* mice to *Rosa26rLacZ* and crossing resulting carriers. We generated *Sox18:GFP-Cre-ErT2(GCE), Cg-Gt(ROSA)26Sor*$^{tm9(CAG-tdTomato)Hze}$*/J* by crossing *Sox18:GFP-Cre-ErT2* mice to *Cg-Gt(ROSA)26Sor*$^{tm9(CAG-tdTomato)Hze}$*/J* homozygous mice. We generated *Pkd1*$^{-/-}$ embryos by crossing *Pkd1*$^{f/f}$ mice to *B6.C-Tg(CMV-cre)1Cgn/J*, and incrossing resulting progeny in subsequent generations. Genotyping primers for *B6.129S4-Pkd1tm2Ggg/J* are described in (Piontek et al., 2004) (F4/R4, F4/R5 combination used).

Imaging and analysis

For live confocal and spinning disk imaging, embryos were mounted as previously described (Hogan et al., 2009b). Imaging was performed in the Australian Cancer Research Foundation's Dynamic Imaging Facility at IMB on a LSM Zeiss 510 NLO, META or Zeiss 710 FCS confocal microscope using a 10X, 20X, 40X dry objective and 63X oil objective. Images were analysed with the Zeiss Zen software, the Biplane IMARIS suite, Photoshop suite and ImageJ.

Morpholino oligomers

Morpholino against *pkd1a* (MO ex8), *pkd1b* (MO ex45) and *pkd2* (MO ATG) were described in (Mangos et al., 2010, Obara et al., 2006) and were injected at 5, 7.5 or 10ng/embryo as described (Hogan et al., 2008).

Quantitative real time PCR

Procedures were performed in order to comply with MIQE guidelines (Bustin et al., 2009) and are given in full in Supplemental Experimental Procedures.

Additional supporting materials and methods are described in Supplemental Experimental Procedures.

Supplementary Material

Refer to Web version on PubMed Central for supplementary material.

Acknowledgments

We thank Christine Neyt, Scott Paterson, Nicole Schieber and Merlijn Witte for technical assistance and Carol Wicking for useful discussions. We thank Holger Gerhardt for providing the GOLPH4 staining protocol, the GUDMAP consortium for providing *Sox18:GCE* and the Baltimore PKD Core Center for providing shRNA against *PKD1*. BMH was funded by an Australian Research Council Future Fellowship (FT100100165), MF by an NHMRC Australia Career Development Fellowship (1011242), and RGP by an NHMRC Australia Fellowship (569542). This work was funded by Cancer Council Queensland project grant (1043659) and in part by NHMRC project grant (631657). Jonathan Astin was funded by the Auckland Medical Research Foundation. Imaging was performed in the Australian Cancer Research Foundation's Dynamic Imaging Facility at IMB.

References

BOCA M, D'AMATO L, DISTEFANO G, POLISHCHUK RS, GERMINO GG, BOLETTA A. Polycystin-1 induces cell migration by regulating phosphatidylinositol 3-kinase-dependent cytoskeletal rearrangements and GSK3beta-dependent cell cell mechanical adhesion. Mol Biol Cell. 2007; 18:4050–61. [PubMed: 17671167]

BOULTER C, MULROY S, WEBB S, FLEMING S, BRINDLE K, SANDFORD R. Cardiovascular, skeletal, and renal defects in mice with a targeted disruption of the Pkd1 gene. Proceedings of the National Academy of Sciences of the United States of America. 2001; 98:12174–12179. [PubMed: 11593033]

BUSSMANN J, BOS FL, URASAKI A, KAWAKAMI K, DUCKERS HJ, SCHULTE-MERKER S. Arteries provide essential guidance cues for lymphatic endothelial cells in the zebrafish trunk. Development (Cambridge, England). 2010; 137:2653–2657.

BUSTIN SA, BENES V, GARSON JA, HELLEMANS J, HUGGETT J, KUBISTA M, MUELLER R, NOLAN T, PFAFFL MW, SHIPLEY GL, VANDESOMPELE J, WITTWER CT. The MIQE guidelines: minimum information for publication of quantitative real-time PCR experiments. Clin Chem. 2009; 55:611–22. [PubMed: 19246619]

CASTELLI M, BOCA M, CHIARAVALLI M, RAMALINGAM H, ROWE I, DISTEFANO G, CARROLL T, BOLETTA A. Polycystin-1 binds Par3/aPKC and controls convergent extension during renal tubular morphogenesis. Nat Commun. 2013; 4:2658. [PubMed: 24153433]

CHAPIN HC, CAPLAN MJ. The cell biology of polycystic kidney disease. J Cell Biol. 2010; 191:701–10. [PubMed: 21079243]

CHEN L, MUPO A, HUYNH T, CIOFFI S, WOODS M, JIN C, MCKEEHAN W, THOMPSON-SNIPES L, BALDINI A, ILLINGWORTH E. Tbx1 regulates Vegfr3 and is required for lymphatic vessel development. J Cell Biol. 2010; 189:417–24. [PubMed: 20439995]

FRANCOIS M, CAPRINI A, HOSKING B, ORSENIGO F, WILHELM D, BROWNE C, PAAVONEN K, KARNEZIS T, SHAYAN R, DOWNES M, DAVIDSON T, TUTT D, CHEAH K, STACKER S, MUSCAT G, ACHEN M, DEJANA E, KOOPMAN P. Sox18 induces development of the lymphatic vasculature in mice. Nature. 2008; 456:643–647. [PubMed: 18931657]

FRANvOIS M, SHORT K, SECKER GA, COMBES A, SCHWARZ Q, DAVIDSON TL, SMYTH I, HONG YK, HARVEY NL, KOOPMAN P. Segmental territories along the cardinal veins generate

lymph sacs via a ballooning mechanism during embryonic lymphangiogenesis in mice. Developmental biology. 2012; 364:89–98. [PubMed: 22230615]

GALVAGNI F, PENNACCHINI S, SALAMEH A, ROCCHIGIANI M, NERI F, ORLANDINI M, PETRAGLIA F, GOTTA S, SARDONE GL, MATTEUCCI G, TERSTAPPEN GC, OLIVIERO S. Endothelial cell adhesion to the extracellular matrix induces c-Src-dependent VEGFR-3 phosphorylation without the activation of the receptor intrinsic kinase activity. Circ Res. 2010; 106:1839–48. [PubMed: 20431062]

GARCIA-GONZALEZ MA, OUTEDA P, ZHOU Q, ZHOU F, MENEZES LF, QIAN F, HUSO DL, GERMINO GG, PIONTEK KB, WATNICK T. Pkd1 and Pkd2 are required for normal placental development. PLoS One. 2010; 5

GENG L, BURROW CR, LI HP, WILSON PD. Modification of the composition of polycystin-1 multiprotein complexes by calcium and tyrosine phosphorylation. Biochim Biophys Acta. 2000; 1535:21–35. [PubMed: 11113628]

HAGERLING R, POLLMANN C, ANDREAS M, SCHMIDT C, NURMI H, ADAMS RH, ALITALO K, ANDRESEN V, SCHULTE-MERKER S, KIEFER F. A novel multistep mechanism for initial lymphangiogenesis in mouse embryos based on ultramicroscopy. EMBO J. 2013; 32:629–44. [PubMed: 23299940]

HASSANE S, CLAIJ N, JODAR M, DEDMAN A, LAURITZEN I, DUPRAT F, KOENDERMAN J, VAN DER WAL A, BREUNING M, DE HEER E, HONORE E, DERUITER M, PETERS D. Pkd1-inactivation in vascular smooth muscle cells and adaptation to hypertension. Lab Invest. 2010

HOGAN B, BOS F, BUSSMANN J, WITTE M, CHI N, DUCKERS H, SCHULTEMERKER S. Ccbe1 is required for embryonic lymphangiogenesis and venous sprouting. Nature genetics. 2009a; 41:396–398. [PubMed: 19287381]

HOGAN B, HERPERS R, WITTE M, HELOTERA H, ALITALO K, DUCKERS H, SCHULTE-MERKER S. Vegfc/Flt4 signalling is suppressed by Dll4 in developing zebrafish intersegmental arteries. Development (Cambridge, England). 2009b; 136:4001–4009.

HOGAN B, VERKADE H, LIESCHKE G, HEATH J. Manipulation of gene expression during zebrafish embryonic development using transient approaches. Methods Mol Biol. 2008; 469:273–300. [PubMed: 19109716]

HUANG P, SCHIER AF. Dampened Hedgehog signaling but normal Wnt signaling in zebrafish without cilia. Development. 2009; 136:3089–98. [PubMed: 19700616]

JAMES JM, NALBANDIAN A, MUKOUYAMA YS. TGFbeta signaling is required for sprouting lymphangiogenesis during lymphatic network development in the skin. Development. 2013; 140:3903–14. [PubMed: 23946447]

JIN SW, BEIS D, MITCHELL T, CHEN JN, STAINIER DY. Cellular and molecular analyses of vascular tube and lumen formation in zebrafish. Development. 2005; 132:5199–209. [PubMed: 16251212]

KARKKAINEN MJ, HAIKO P, SAINIO K, PARTANEN J, TAIPALE J, PETROVA TV, JELTSCH M, JACKSON DG, TALIKKA M, RAUVALA H, BETSHOLTZ C, ALITALO K. Vascular endothelial growth factor C is required for sprouting of the first lymphatic vessels from embryonic veins. Nature immunology. 2004; 5:74–80. [PubMed: 14634646]

KARTOPAWIRO J, BOWER NI, KARNEZIS T, KAZENWADEL J, BETTERMAN KL, LESIEUR E, KOLTOWSKA K, ASTIN J, CROSIER P, VERMEREN S, ACHEN MG, STACKER SA, SMITH KA, HARVEY NL, FRANCOIS M, HOGAN BM. Arap3 is dysregulated in a mouse model of hypotrichosis-lymphedema-telangiectasia and regulates lymphatic vascular development. Hum Mol Genet. 2013

KIM K, DRUMMOND I, IBRAGHIMOV-BESKROVNAYA O, KLINGER K, ARNAOUT MA. Polycystin 1 is required for the structural integrity of blood vessels. Proceedings of the National Academy of Sciences of the United States of America. 2000; 97:1731–1736. [PubMed: 10677526]

KOLTOWSKA K, BETTERMAN KL, HARVEY NL, HOGAN BM. Getting out and about: the emergence and morphogenesis of the vertebrate lymphatic vasculature. Development. 2013; 140:1857–70. [PubMed: 23571211]

KUCHLER A, GJINI E, PETERSON-MADURO J, CANCILLA B, WOLBURG H, SCHULTE-MERKER S. Development of the zebrafish lymphatic system requires VEGFC signaling. Curr Biol. 2006; 16:1244–1248. [PubMed: 16782017]

LAL M, SONG X, PLUZNICK JL, DI GIOVANNI V, MERRICK DM, ROSENBLUM ND, CHAUVET V, GOTTARDI CJ, PEI Y, CAPLAN MJ. Polycystin-1 C-terminal tail associates with beta-catenin and inhibits canonical Wnt signaling. Hum Mol Genet. 2008; 17:3105–17. [PubMed: 18632682]

LAWSON ND, WEINSTEIN BM. In vivo imaging of embryonic vascular development using transgenic zebrafish. Developmental biology. 2002; 248:307– 318. [PubMed: 12167406]

LE GUEN L, KARPANEN T, SCHULTE D, HARRIS NC, KOLTOWSKA K, ROUKENS G, BOWER NI, VAN IMPEL I, STACKER SA, ACHEN MG, SCHULTE-MERKER S, HOGAN BM. Ccbe1 regulates Vegfc-mediated induction of Vegfr3 signaling during embryonic lymphangiogenesis. Development. 2014; 141:1239–49. [PubMed: 24523457]

MÄKINEN T, JUSSILA L, VEIKKOLA T, KARPANEN T, KETTUNEN MI, PULKKANEN KJ, KAUPPINEN R, JACKSON DG, KUBO H, NISHIKAWA S, YLÄ-HERTTUALA S, ALITALO K. Inhibition of lymphangiogenesis with resulting lymphedema in transgenic mice expressing soluble VEGF receptor-3. Nature medicine. 2001; 7:199–205.

MANGOS S, LAM P, ZHAO A, LIU Y, MUDUMANA S, VASILYEV A, LIU A, DRUMMOND I. The ADPKD genes pkd1a/b and pkd2 regulate extracellular matrix formation. Dis Model Mech. 2010; 3:354–365. [PubMed: 20335443]

MUTO S, AIBA A, SAITO Y, NAKAO K, NAKAMURA K, TOMITA K, KITAMURA T, KURABAYASHI M, NAGAI R, HIGASHIHARA E, HARRIS PC, KATSUKI M, HORIE S. Pioglitazone improves the phenotype and molecular defects of a targeted Pkd1 mutant. Hum Mol Genet. 2002; 11:1731–42. [PubMed: 12095915]

NAULI SM, ALENGHAT FJ, LUO Y, WILLIAMS E, VASSILEV P, LI X, ELIA AE, LU W, BROWN EM, QUINN SJ, INGBER DE, ZHOU J. Polycystins 1 and 2 mediate mechanosensation in the primary cilium of kidney cells. Nat Genet. 2003; 33:129–37. [PubMed: 12514735]

NAULI SM, KAWANABE Y, KAMINSKI JJ, PEARCE WJ, INGBER DE, ZHOU J. Endothelial cilia are fluid shear sensors that regulate calcium signaling and nitric oxide production through polycystin-1. Circulation. 2008; 117:1161–1171. [PubMed: 18285569]

NORTH TE, GOESSLING W, PEETERS M, LI P, CEOL C, LORD AM, WEBER GJ, HARRIS J, CUTTING CC, HUANG P, DZIERZAK E, ZON LI. Hematopoietic stem cell development is dependent on blood flow. Cell. 2009; 137:736–748. [PubMed: 19450519]

OBARA T, MANGOS S, LIU Y, ZHAO J, WIESSNER S, KRAMER-ZUCKER AG, OLALE F, SCHIER AF, DRUMMOND IA. Polycystin-2 immunolocalization and function in zebrafish. Journal of the American Society of Nephrology: JASN. 2006; 17:2706–2718. [PubMed: 16943304]

OKUDA KS, ASTIN JW, MISA JP, FLORES MV, CROSIER KE, CROSIER PS. lyve1 expression reveals novel lymphatic vessels and new mechanisms for lymphatic vessel development in zebrafish. Development (Cambridge, England). 2012

PIONTEK KB, HUSO DL, GRINBERG A, LIU L, BEDJA D, ZHAO H, GABRIELSON K, QIAN F, MEI C, WESTPHAL H, GERMINO GG. A functional floxed allele of Pkd1 that can be conditionally inactivated in vivo. Journal of the American Society of Nephrology: JASN. 2004; 15:3035–3043. [PubMed: 15579506]

ROITBAK T, WARD CJ, HARRIS PC, BACALLAO R, NESS SA, WANDINGER-NESS A. A polycystin-1 multiprotein complex is disrupted in polycystic kidney disease cells. Molecular biology of the cell. 2004; 15:1334–1346. [PubMed: 14718571]

ROSSETTI S, HARRIS PC. The genetics of vascular complications in autosomal dominant polycystic kidney disease (ADPKD). Curr Hypertens Rev. 2013; 9:37–43. [PubMed: 23971643]

SCHWENK F, BARON U, RAJEWSKY K. A cre-transgenic mouse strain for the ubiquitous deletion of loxP-flanked gene segments including deletion in germ cells. Nucleic Acids Res. 1995; 23:5080–1. [PubMed: 8559668]

SRINIVASAN R, GENG X, YANG Y, WANG Y, MUKATIRA S, STUDER M, PORTO M, LAGUTIN O, OLIVER G. The nuclear hormone receptor Coup-TFII is required for the initiation

and early maintenance of Prox1 expression in lymphatic endothelial cells. Genes & development. 2010; 24:696–707. [PubMed: 20360386]

TATIN F, TADDEI A, WESTON A, FUCHS E, DEVENPORT D, TISSIR F, MAKINEN T. Planar cell polarity protein Celsr1 regulates endothelial adherens junctions and directed cell rearrangements during valve morphogenesis. Dev Cell. 2013; 26:31–44. [PubMed: 23792146]

VILLEFRANC JA, NICOLI S, BENTLEY K, JELTSCH M, ZARKADA G, MOORE JC, GERHARDT H, ALITALO K, LAWSON ND. A truncation allele in vascular endothelial growth factor c reveals distinct modes of signaling during lymphatic and vascular development. Development. 2013; 140:1497–506. [PubMed: 23462469]

WANG Y, NAKAYAMA M, PITULESCU ME, SCHMIDT TS, BOCHENEK ML, SAKAKIBARA A, ADAMS S, DAVY A, DEUTSCH U, LUTHI U, BARBERIS A, BENJAMIN LE, MAKINEN T, NOBES CD, ADAMS RH. Ephrin-B2 controls VEGF-induced angiogenesis and lymphangiogenesis. Nature. 2010; 465:483–6. [PubMed: 20445537]

WIGLE JT, OLIVER G. Prox1 function is required for the development of the murine lymphatic system. Cell. 1999; 98:769–778. [PubMed: 10499794]

YANG Y, GARCIA-VERDUGO JM, SORIANO-NAVARRO M, SRINIVASAN RS, SCALLAN JP, SINGH MK, EPSTEIN JA, OLIVER G. Lymphatic endothelial progenitors bud from the cardinal vein and intersomitic vessels in mammalian embryos. Blood. 2012; 120:2340–8. [PubMed: 22859612]

YANIV K, ISOGAI S, CASTRANOVA D, DYE L, HITOMI J, WEINSTEIN B. Live imaging of lymphatic development in the zebrafish. Nature medicine. 2006; 12:711–716.

YUAN L, MOYON D, PARDANAUD L, BREANT C, KARKKAINEN MJ, ALITALO K, EICHMANN A. Abnormal lymphatic vessel development in neuropilin 2 mutant mice. Development. 2002; 129:4797–806. [PubMed: 12361971]

ZHOU J. Polycystins and primary cilia: primers for cell cycle progression. Annual review of physiology. 2009; 71:83–113.

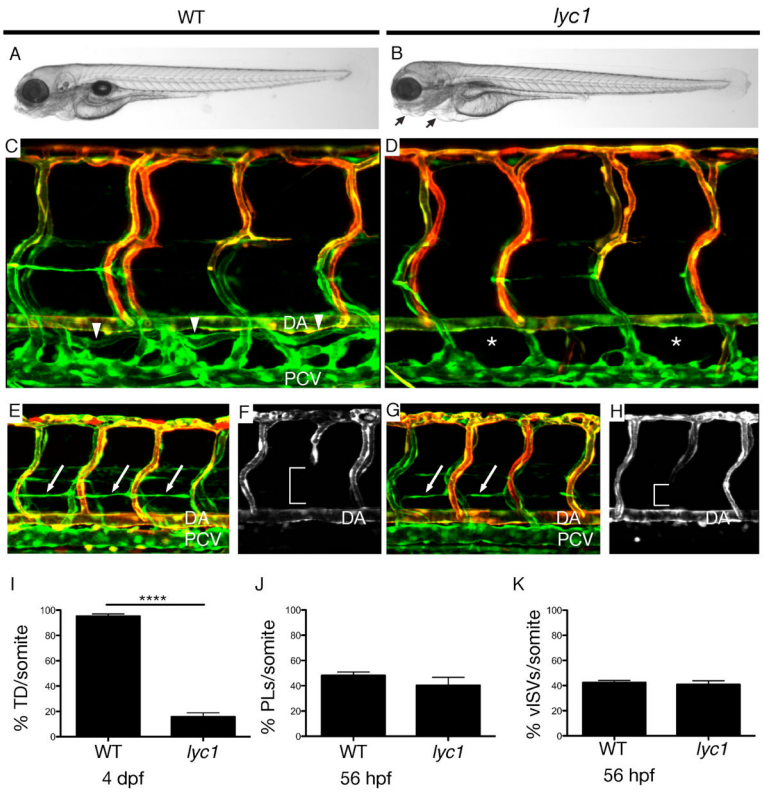

Figure 1. lyc1 mutants display reduced lymphatic development

(**A–B**) Overall morphology of wildtype siblings (**A**) and *lyc1* mutants (**B**) at 4 dpf.

(**C–D**) The vasculature Tg(*fli1a:EGFP*^{y1}*; flt1:tomato*^{hu5333Tg}) of (**C**) WT (arrowheads indicate thoracic duct) and (**D**) *lyc1* mutants at 4 dpf (asterix indicate absence of thoracic duct).

(**E,G**) The vasculature Tg(*fli1a:EGFP*^{y1}*; flt1:tomato*^{hu5333Tg}) in wildtype sibling (**E**) and mutant embryos (**G**) at 56 hpf (arrows indicate lymphatic precursors known as parachordal lymphangioblasts, PLs).

(**F,H**) *flt1:tomato*^{hu5333Tg} expression marks the arterial ECs, a loss of signal (brackets) indicating venous intersegmental vessels (vISV).

(**I–K**) Quantification of (**I**) thoracic duct extent across 10 somites (WT n=40, *lyc1* n=17), **(J)** parachordal lymphangioblasts (WT n=78, *lyc1* n=17) and (**K**) venous sprouts (WT n=40, *lyc1* n=15). DA: dorsal aorta, PCV: posterior cardinal vein.

See also Figure S1, S2, S3.

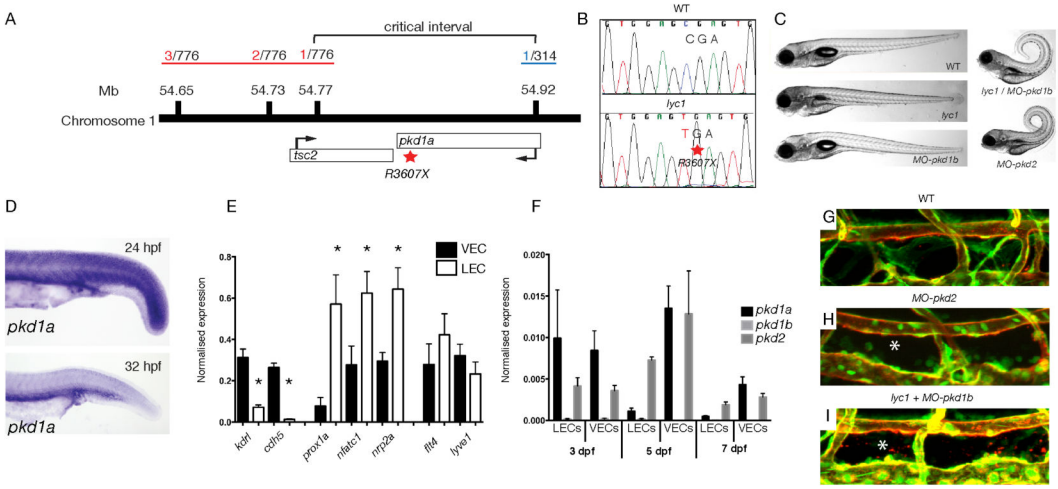

Figure 2. *lyc1* is a *pkd1a* mutant

(A) Overview of positional cloning of *lyc1*. Individual recombinant embryos (labeled in red left (from 776 embryos analysed), labeled in blue right (from 314 embryos analysed)) identify flanking polymorphic markers and limit the critical interval to a region containing partial sequences for *pkd1a* and *tsc2*.

(B) Sequence chromatograms showing the wildtype (upper) and *pkd1a* mutant (R3607X, lower) sequences.

(C) Overall morphology of 5 dpf WT, *lyc1, MO-pkd1b*, *lyc1/MO-pkd1b* and *MO-pkd2* embryos. The injection of *MO-pkd1b* into *lyc1* mutants recapitulates the published *MO-pkd1a/1b* double loss-of-function phenotype (Mangos et al., 2010).

(D) Expression pattern of *pkd1a* by *in situ* hybridisation in the trunk of wild type zebrafish at 24hpf and 32hpf.

(E) Quantitative RT PCR for markers enriched in venous endothelial cells (VECs); *kdrl*, *cdh5,* LECs; *prox1a*, *nfatc1*, *nrp2a*, and both; *flt4, lyve1* demonstrated the purity of FACs isolated populations at 5 dpf

(F) Quantitative RT PCR for *pkd1a, pkd1b* and *pkd2* transcripts in 3, 5 and 7 dpf VEC and LEC populations.

(G–I) The vasculature of 5 dpf WT, *lyc1/MO-pkd1b* and *MO-pkd2* embryos (5 and 7.5ng MO respectively), asterix indicates absence of thoracic duct in Tg(*fli1a:EGFP*^{y1}*; kdrl:egfp*^{s843}*)* embryos.

See also Figure S4, S5.

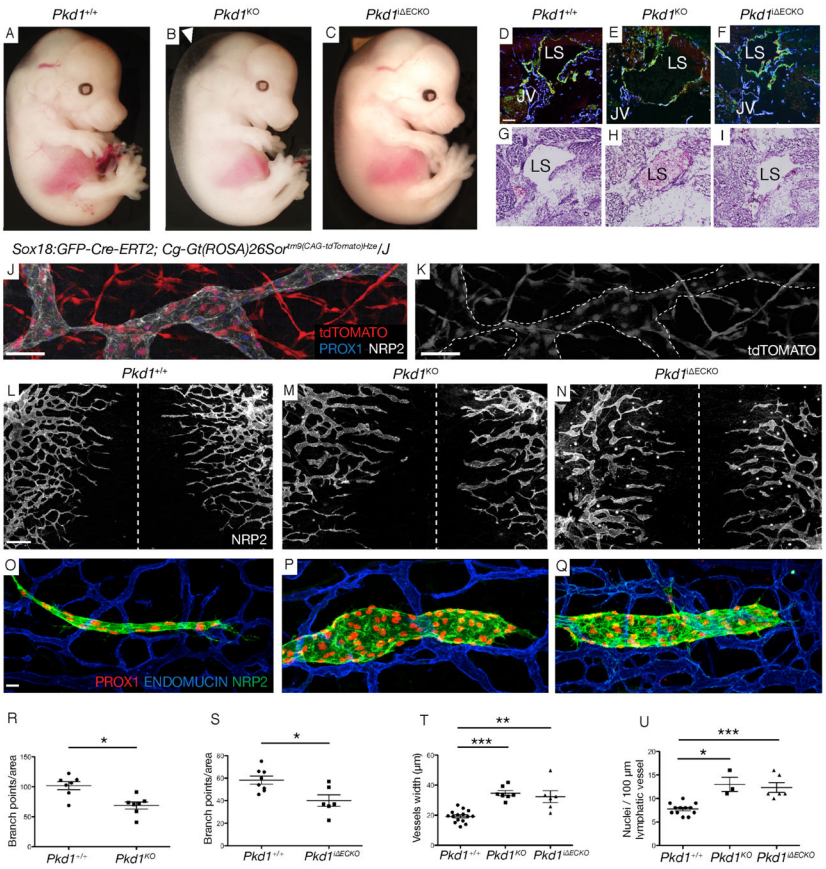

Figure 3. *Pkd1* cell-autonomously regulates subcutaneous lymphatic vascular development in mice

(A–C) Morphology of WT, *Pkd1*^{KO} and *Pkd1*$^{i\Delta ECKO}$ embryos at 14.5 dpc (arrowhead indicates oedema).

(**D–F)** Lymph sacs (LS) in WT, *Pkd1*^{KO} and *Pkd1*$^{i\Delta ECKO}$ embryos stained with ENDOMUCIN, LYVE1 and PROX1. JV=Jugular vein. Scale bar: 100 µm

(**G–I**) Hematoxylin and eosin staining in WT, *Pkd1*^{KO}, *Pkd1*$^{i\Delta ECKO}$ embryos at 14.5 dpc,. Lymph sacs (LS) indicated.

(**J–K**) Subcutaneous lymphatics in *Sox18:GFP-Cre-ERT2, Cg-Gt(ROSA)26Sor*$^{tm9(CAG\text{-}tdTomato)Hze}$*/J* co-stained with NRP2 and PROX1 (n=663/1138 scored LECs were tdTOMATO positive (58.2%), from n=2 embryos, 13.5 dpc).

(**L–N**) Subcutaneous lymphatic vasculature in WT, *Pkd1*^{KO} and *Pkd1*$^{\Delta ECKO}$ mutants at 14.5 dpc. Hashed line indicated the dorsal midline of the embryo. Scale bar: 400 µm

(O–Q) Representative subcutaneous lymphatic sprout in WT, *Pkd1*^{KO} and *Pkd1*$^{i\Delta ECKO}$ mutants at 14.5 dpc.

(R,S) Quantification of branch points/area (2000*1500 µm area on both sides of the midline) in (**R**) WT (n=7 embryos) and *Pkd1*^{KO} (n=7 embryos) and (**S**) WT (n=8 embryos) and *Pkd1*$^{i\Delta ECKO}$ (n=6 embryos) embryos at 14.5 dpc.

(T) Quantification of the average width of lymphatic vessels (µm) across the whole skin in WT (n=15 embryos), *Pkd1*^{KO} (n=7 embryos) and *Pkd1*$^{i\Delta ECKO}$ (n=6 embryos) embryos. The

average is shown of n=773, n=354 and n=250 measurements respectively, across leading lymphatic vessels from both sides of the midline at 14.5 dpc.

(U) Quantification of nuclei/100 μm of vessel in WT (n=12 embryos), $Pkd1^{KO}$ (n=3 embryos) and $Pkd1^{i\Delta ECKO}$ (n=6 embryos) (n=5 representative leading edge vessels counted per embryo) at 14.5 dpc.

See also Figure S6. S7, S8.

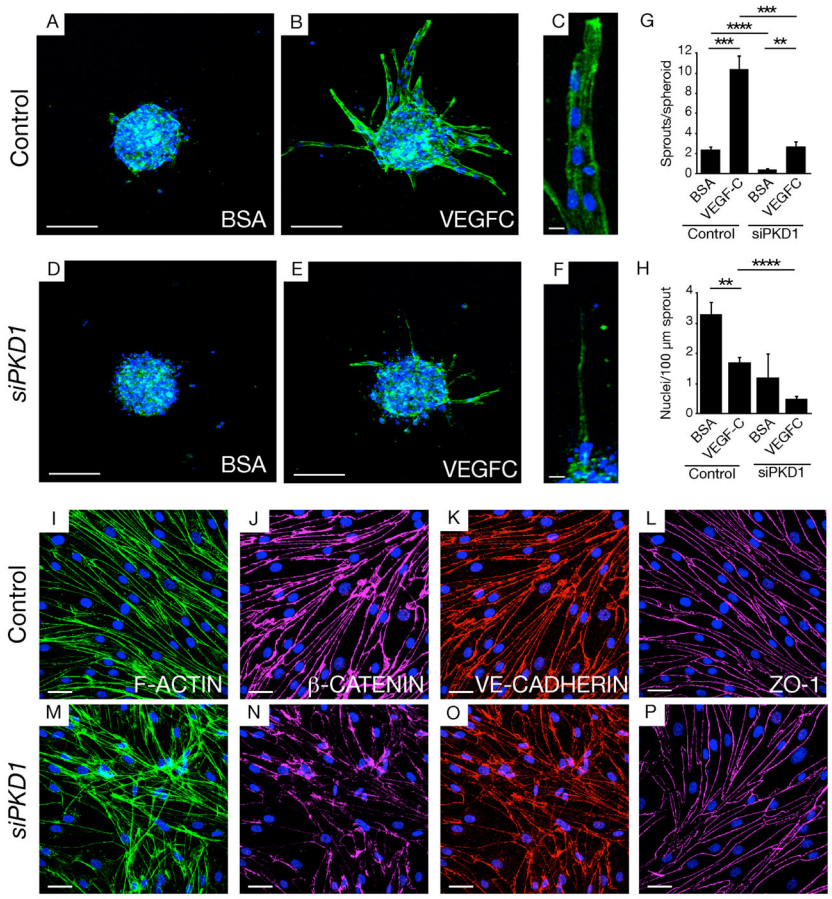

Figure 4. PKD1 regulates sprouting and cell-cell junctions in LECs *in vitro*

(**A–F**) Morphology of human LEC spheroids treated with control and *PKD1* siRNA (50nM) in BSA or VEGFC supplemented conditions, stained with F-ACTIN (green) and DAPI (blue). Scale bar: 100 μm (**A, B, D, E**), 30 μm (**C, F**).

(**G–H**) Quantification of number of sprouts (**G**) and number of nuclei per 100 μm of sprouts (**H**) in spheroids treated with control of *PKD1* siRNA in BSA or VEGFC supplemented conditions.

(**I–P**) Morphology of human LECs treated with control and *PKD1* siRNA (50nM) VEGFC supplemented conditions, stained with DAPI (blue) and F-ACTIN (green) (**I,M**), β-CATENIN (pink) (**J,N**), VE-CADHERIN (red) (**K,O**) or ZO-1 (**L,P**).

See also Figure S9.

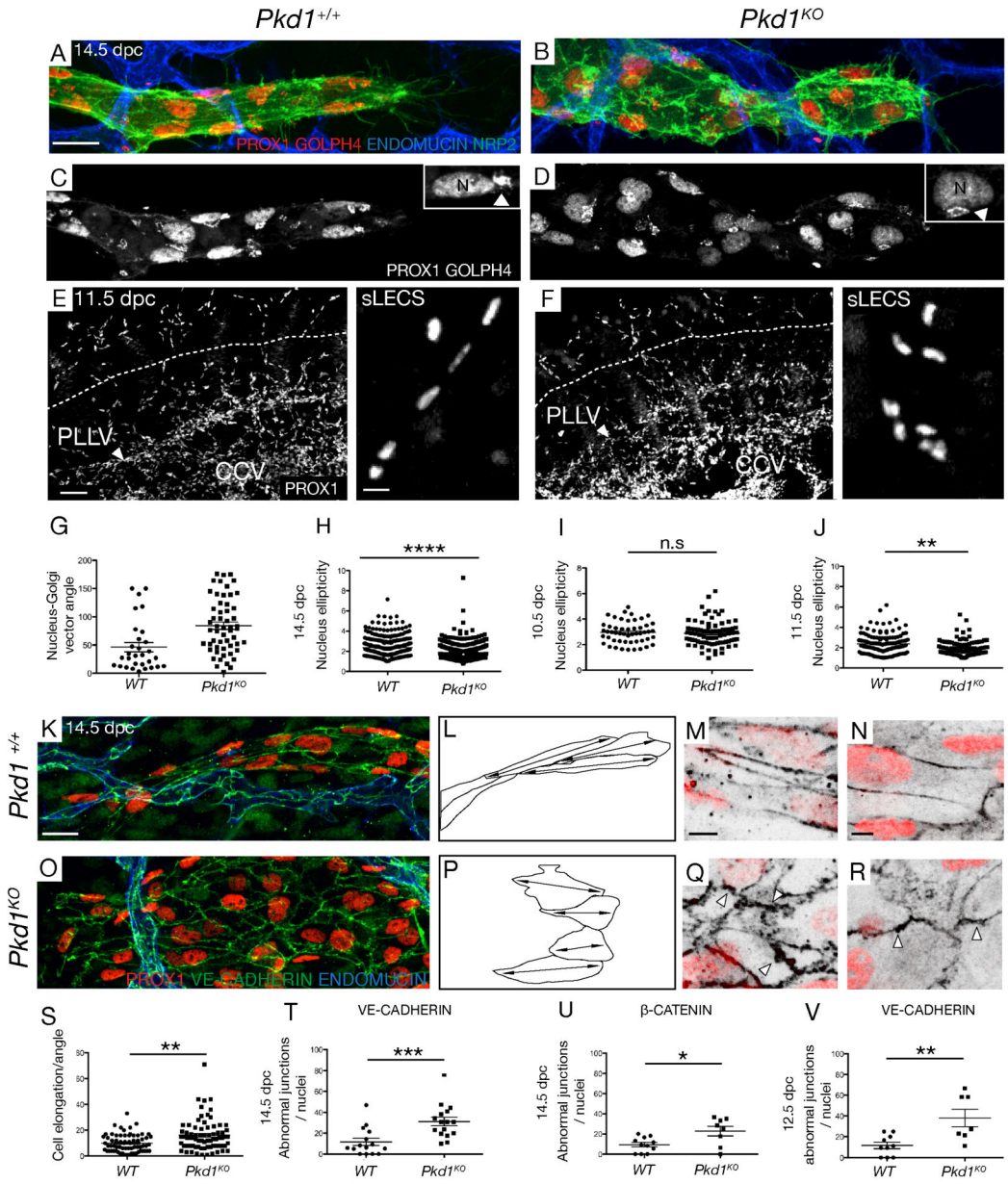

Figure 5. *Pkd1* regulates polarity and cell-cell junctions in mouse embryonic lymphatic vessels

(A,B) Subcutaneous lymphatic vessels in skin in WT and *Pkd1*^{KO} embryos at 14.5 dpc, stained with ENDOMUCIN, NRP2, PROX1 and GOLPH4 (golgi apparatus), non-LEC staining subtracted.. Scale bar: 20 μm

(C,D) PROX1, GOLPH4 staining in WT and *Pkd1*^{KO} lymphatic vessels. Arrowhead indicates Golgi, N=nucleus.

(**E, F**) Lateral view of (**E**) WT (n=3) and (**F**) *Pkd1*^{KO} (n=2) bisected embryos with PROX1 at 11.5 dpc. CCV=common cardinal vein. Right panels show morphology of migrating sLEC nuclei (analysed above dashed line). Scale bar: 50 μm (10 μm in right hand panels)

(G–H) Quantification of nucleus-golgi vector angle (**G**) in WT (n=3 embryos, n=30 nuclei) and *Pkd1*^{KO} (n=4, n=55 nuclei) and (**H**) quantification of nucleus sphericity (width to length ratio) in WT (n=7, n=299 nuclei) and *Pkd1*^{KO} (n=7, n=498 nuclei) at 14.5 dpc.
(**I–J**) Quantification of nucleus sphericity in (**I**) dorsal-most iLECs in WT (n=5, n=51 nuclei) versus *Pkd1*^{KO} (n=5, n=79 nuclei) embryos at 10.5 dpc, (**J**) in sLECs in WT (n=3, n=131 nucleus) and *Pkd1*^{KO} (n=2, n=93 nucleus) embryos at 11.5 dpc
(**K, O**) Representative subcutaneous lymphatic vessels in (**K**) WT and (**O**) *Pkd1*^{KO} embryos stained with ENDOMUCIN, PROX1 and VE-CADHERIN at 14.5 dpc. Scale bar: 20 μm
(**L, P**) Representative cell shape schematics based on vessels shown in **K** and **O**, show abnormal elongation in the direction of vessel migration. Double sided arrows indicate elongation axes.
(**M, Q**) WT and *Pkd1*^{KO} mutant cells at 14.5 dpc stained with PROX1 and VE-CADHERIN. Arrowheads indicate abnormal junctional protrusions. Scale bar: 5 μm
(**N, R**) WT and *Pkd1*^{KO} mutant cells at 14.5 dpc stained with PROX1 and β-CATENIN. Arrowheads indicate abnormal junctional protrusions. Scale bar: 5 μm
(**S**) Quantification of the angle of cell elongation relative to the direction of migration in WT (n=68 cells, n=4 embryos) and *Pkd1*^{KO} (n=74 cells, n=4 embryos).
(T) Quantification of the average number of cells with abnormal junctions (stained with VE-CADHERIN) per nuclei in WT (n=4 embryos, n= 15 vessels) and *Pkd1*^{KO} (n=4 embryos, n= 16 vessels) at 14.5 dpc.
(**U**) Quantification of abnormal junctions (stained with β-CATENIN) in WT (n=3 embryos, n=11 vessels) and *Pkd1*^{KO} (n=2 embryos, n=8 vessels) at 14.5 dpc.
(**V**) Quantification of the average number of cells with abnormal junctions (stained with VE-CADHERIN) per nuclei in WT (n=4 embryos, n=10 vessels) and *Pkd1*^{KO} (n=3 embryos, n=7 vessels) at 12.5 dpc.
iLECS: initial LECs, PLLV: peripheral longitudinal lymphatic vessel, sLECS: superficial LECs. CCV: Common cardinal vein.